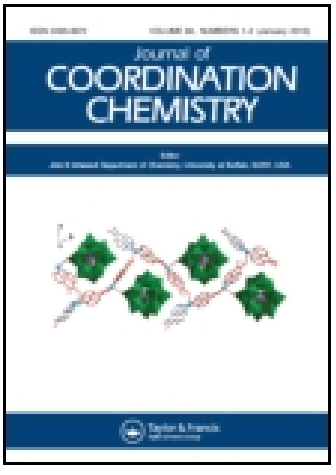

Journal of Coordination Chemistry
Publication details, including instructions for authors and subscription information:
http://www.tandfonline.com/loi/gcoo20

Synthesis, characterization, photoluminescent properties and supramolecular aggregations in diimine chelated cadmium dihalides

Tushar S. Basu Baul[a], Sajal Kundu[a], Seik Weng Ng[bc], Nikhil Guchhait[d] & Edward R.T. Tiekink[b]

[a] Department of Chemistry, North-Eastern Hill University, Shillong, India

[b] Department of Chemistry, University of Malaya, Kuala Lumpur, Malaysia

[c] Department of Chemistry, King Abdulaziz University, Jeddah, Saudi Arabia

[d] Department of Chemistry, University of Calcutta, Kolkata, India

Accepted author version posted online: 13 Nov 2013.Published online: 23 Dec 2013.

To cite this article: Tushar S. Basu Baul, Sajal Kundu, Seik Weng Ng, Nikhil Guchhait & Edward R.T. Tiekink (2014) Synthesis, characterization, photoluminescent properties and supramolecular aggregations in diimine chelated cadmium dihalides, Journal of Coordination Chemistry, 67:1, 96-119, DOI: 10.1080/00958972.2013.864393

To link to this article: http://dx.doi.org/10.1080/00958972.2013.864393

Journal of Coordination Chemistry, 2014
Vol. 67, No. 1, 96–119, http://dx.doi.org/10.1080/00958972.2013.864393

Synthesis, characterization, photoluminescent properties and supramolecular aggregations in diimine chelated cadmium dihalides

TUSHAR S. BASU BAUL*†, SAJAL KUNDU†, SEIK WENG NG‡§, NIKHIL GUCHHAIT¶ and EDWARD R.T. TIEKINK*‡

†Department of Chemistry, North-Eastern Hill University, Shillong, India
‡Department of Chemistry, University of Malaya, Kuala Lumpur, Malaysia
§Department of Chemistry, King Abdulaziz University, Jeddah, Saudi Arabia
¶Department of Chemistry, University of Calcutta, Kolkata, India

(*Received 29 August 2013; accepted 31 October 2013*)

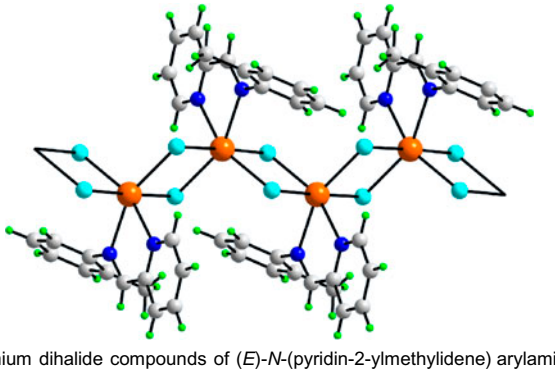

Cadmium dihalide compounds of (*E*)-*N*-(pyridin-2-ylmethylidene) arylamines can be tailored to be monomeric, dimeric and polymeric.

A series of 12 new cadmium compounds, $[Cd(X_2)(L)]$ (**4**, **10**), $[Cd(X_2)(L)(DMSO)]$ (**9**), $[Cd(X_2)(L)]_2$ (**1–3**, **5**, **7**, **8**, **11**, and **12**), and $[Cd(Cl_2)_2(L)]_n$ (**6**) where X = chloride, bromide, and iodide, and diimine L = (*E*)-*N*-(pyridin-2-ylmethylidene)arylamine, were synthesized and characterized by elemental analyses. The spectroscopic properties were investigated by IR, UV–Vis, fluorescence, and ^{1}H NMR studies. The solid-state structures of the 12 reaction products were studied by X-ray crystallography. A majority of the structures are binuclear with five-coordinate cadmium centers: dimerization occurs through μ_2-bridging of the respective halides; the second halide is bound terminally. In the case of X = Br and I, dimerization is circumvented when L carries an additional donor capable of coordinating cadmium (**4**, **10**) or when the additional donor is provided by coordinating solvent (**9**). A similar situation pertains in the $CdCl_2$ analog (**7**). In the case where L strongly coordinates with cadmium, i.e. (**6**), an edge-shared polymeric chain and octahedrally coordinated cadmium are found as a result of μ_2-bridging of both chloro ligands. An interesting feature of the crystal packing is the observation of rare C–H…π interactions where the π-system is a chelate ring or a Cd_2Br_2 unit.

Keywords: Cadmium; (*E*)-*N*-(pyridin-2-ylmethylidene)arylamine; *N,N*-Donor ligands; Spectroscopy; Structure elucidation; Supramolecular aggregations

*Corresponding authors. Emails: basubaul@nehu.ac.in, basubaulchem@gmail.com (T.S. Basu Baul); Edward.Tiekink@gmail.com, Edward.Tiekink@um.edu.my (E.R.T. Tiekink)

1. Introduction

Iminopyridyl-based ligands and metal complexes have found increasing application as catalyst precursors in olefin polymerization following the discovery by Brookhart, Bennett, and Gibson that five-coordinate 2,6-bis(arylimino)pyridyl metal dihalides (particularly Fe and Co complexes), upon activation with methylaluminoxane, are efficient catalysts [1]. First and second row late-transition metal halide (Fe, Co, Ni, Cu, Pd) complexes of bidentate (*N*,*N*′) (imino)pyridines show promising catalytic results; cobalt(II) complexes were better performers in terms of activity for the oligomerization of ethylene to short-chain α-olefins (C4–C12) [2–6]. Recently, the correlation of the structure of these (imino)pyridyl (*N*,*N*′) metal complexes with their use as catalyst precursors for the homopolymerization, oligomerization, and copolymerization of olefins has been described [7].

Construction of coordination networks by self-assembly has attracted considerable attention in supramolecular chemistry and crystal engineering, owing to their potential applications in gas storage [8, 9], photoluminescence [10, 11], catalysis [12–15], magnetism [16], and molecular sensing [17, 18]. Supramolecular structures are affected by the structure of ligands [19–22], the coordination geometry of metal ions [23], counter-anions [24–27], hydrogen bonds [28–31], π–π stacking [32], etc.; among these, anions play a very important role in the self-assembled construction. Metal complexes of chelating pyridine and diimines continues to draw general interest in coordination chemistry and consequently they were also investigated along with cadmium halides to afford complexes of compositions $[Cd(\mu\text{-}X)_2(L)_2]$, $[Cd(\mu\text{-}X)_2(L)_2]^1_\infty$ (X = Cl, Br, I; L = monodentate N-donor ligands, e.g. pyridine and derivatives) and $[Cd(\mu\text{-}X)_2(4,4'\text{-bipyridine})]^2_\infty$ (X = Cl, Br, I). Mononuclear tetrahedral compounds are obtained when the most sterically demanding ligands are present, e.g. I and 3,5-dimethylpyridine, while in all other cases 1- or 2-D coordination polymers are observed [33]. In the polymeric chains, cadmium(II) cations are linked in an edge-sharing fashion by halide bridges in their pseudo-equatorial plane, with terminal pyridine ligands completing the pseudo-octahedral coordination sphere [33, 34]. The effects of anion upon cadmium compounds containing chelating 2,2′-bipyridine (bipy) ligands have been studied recently and in each instance a different structural type has been encountered, e.g. $[Cd(\mu\text{-}Cl)_2(bipy)]_\infty$, $[Cd(Br/I)_2(bipy)_2]$, $[Cd(NO_3)_2(bipy)_2]$, $[Cd(NO_3)(bipy)_2(H_2O)](NO_3)$, $[Cd(bipy)_3](ClO_4)_2$, and $[Cd(O_2CPh)_2bipy(H_2O)]\cdot(H_2O)$ where the coordination geometry of cadmium atom is a distorted octahedral [35]. Among these, $[Cd(O_2CPh)_2(bipy)(H_2O)]\cdot(H_2O)$ was found to efficiently catalyze the transesterification of a variety of esters with methanol [36]. Underscoring the importance of reaction conditions, when the aforementioned $[Cd(I)_2(bipy)_2]$ compound was prepared by a hydrothermal route [36], the same distorted octahedral geometry was revealed but now within a monoclinic (*C*2/*c*) polymorph as opposed to the original orthorhombic (*Pbcn*) form [35]. The coordinating properties of ambidentate ligand 5,5′-diamino-2,2′-bipyridine (5,5′-diamino-2,2′-bipy) towards cadmium were investigated with the desire to generate tetrahedral or octahedral building blocks for supramolecular assemblies based on chelation. The cadmium compound $[Cd(\mu\text{-}Cl)_2(5,5'\text{-diamino-}2,2'\text{-bipy}]^1_\infty$ forms 1-D polymeric strands constructed by bridging chloro ligands and contains distorted octahedral cadmium centers comprising two nitrogens of 5,5′-diamino-2,2′-bipy and four bridging chlorides [37]. A similar coordination geometry around cadmium was observed in the structure of 1,10-phenanthroline (phen) compound $[Cd(\mu\text{-}Cl)_2phen]_\infty$ which expands into a chain through the μ_2-bridging of the chloro ligands [38]. Owing to the presence of the large lateral aromatic phen ligand, the chains associate via a strong π...π stacking interactions, resulting in a zipper-like, double-stranded chain

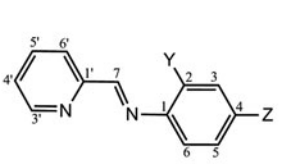

L^1 Y = Z = H
L^2 Y = Me, Z = H
L^3 Y = H, Z = Me
L^4 Y = OMe, Z = H
L^5 Y = H, Z = OMe
L^6 Y = H, Z = Cl

6	$[Cd(Cl)_2(L^2)]_n$	**1**	$[Cd(Br)_2(L^1)]_2$	**8**	$[Cd(I)_2(L^3)]_2$
7	$[Cd(Cl)_2(L^6)]_2$	**2**	$[Cd(Br)_2(L^2)]_2.C_6H_6$	**9**	$[Cd(I)_2(L^3)(DMSO)]$
		3	$[Cd(Br)_2(L^3)]_2$	**10**	$[Cd(I)_2(L^4)]$
		4	$[Cd(Br)_2(L^4)]$	**11**	$[Cd(I)_2(L^5)]_2$
		5	$[Cd(Br)_2(L^5)]_2.2CH_3CN$	**12**	$[Cd(I)_2(L^6)]_2$

Chart 1. Chemical structures of molecules L^1–L^6 and formulation of cadmium(II) compounds **1–12**.

[39]. The structures of bis(phen) compounds, e.g. $[Cd(X)_2(phen)_2]$ where X = Cl [40] and Br [41], are also known and the crystal packing of $[Cd(Br)_2(phen)_2]$ is stabilized by intermolecular π…π and C–H…Br interactions [41]. Ionic compounds of cadmium and bipy were also prepared and shown to have diverse compositions, e.g. $[Cd(bipy)_3][PF_6]_2$ [42], $[Cd(bipy)_2(H_2O)(ClO_4)][ClO_4]$, $[Cd(bipy)_3][ClO_4]_2 \cdot 0.5bipy$ [43], $[Cd(bipy)_3][ClO_4]_2 \cdot 0.5H_2O$ [44], a hydrothermal product $[Cd(phen)_2(H_2O)_2]SO_4 \cdot 6H_2O$ [45], and a bipy derivative $[Cd(3,3'\text{-diamino-bipy})_3][NO_3]_2$ [46]; each has a distorted octahedral geometry around the cadmium atom.

We are recently engaged in a program to investigate the coordination behavior of (*E*)-N-(pyridin-2-ylmethylidene)arylamines (L), which differ in the nature and location of substituents in the aryl ring towards the zinc-triad elements with different anions. With mercury(II), four types of neutral compounds were generated of formulae: $[Hg(X)_2L]$, $[Hg(\mu\text{-}X)_2L]$, $[Hg(\mu\text{-}NO_3)(NO_3)L]_n$[1], and $\{[Hg(\mu\text{-}N_3)_2L]_2\}_n$[1] [47]. In view of the observed structural diversity in the mercury(II) structures, attention was directed towards cadmium (II). Herein, five dibromo compounds with compositions $[Cd(Br)_2(L^n)]_2$ (**1–3**, **5**) and $[Cd(Br)_2(L^n)]$ (**4**), two dichloro compounds $[Cd(Cl)_2(L^n)]_n$ (**6**) and $[Cd(Cl)_2(L^n)]_2$ (**7**), and five diiodo compounds $[Cd(I)_2(L^n)]_2$ (**8**, **11**, **12**), $[Cd(I)_2(L^n)(DMSO)]$ (**9**) and $[Cd(I)_2(L^n)]$ (**10**) are described (refer to chart 1 for chemical structures of L^n). Compounds **1–12** have been characterized by IR and ^1H NMR spectroscopic studies, and the solution and solid-state photophysical properties are also discussed. Detailed structural information has been afforded by single-crystal X-ray crystallographic analyses.

2. Experimental

2.1. *Materials and physical measurements*

All chemicals were used as purchased without purification: $CdCl_2$ (Sarabhai chemicals), $CdBr_2$ (Sigma Aldrich), CdI_2 (Sisco Research laboratories), aniline (Sd Fine), *o*-toluidine (Thomas Bakers), *p*-toluidine (CDH), *o*-anisidine and *p*-anisidine (CDH), *p*-chloroaniline (HiMedia), and pyridine-2-carboxaldehyde (Merck). Solvents were purified by standard procedures and freshly distilled prior to use. The (*E*)-*N*-(pyridin-2-ylmethylidene)arylamines derivatives, L^1–L^6, were prepared *in situ* from pyridine-2-carboxaldehyde and the

corresponding aniline [47]. Elemental analyses, solution electrical conductivity measurements, IR, ^{1}H NMR, and UV–vis spectra were recorded on instruments and under conditions as described elsewhere [47]. Fluorescence spectra were obtained on a Hitachi model FL4500 spectrofluorimeter (with the excitation and emission slits fixed at 10 and 20 nm, respectively) and all spectra were corrected for the instrument response function and conditions as described earlier [47]. Solid-state fluorescence spectra were obtained using a Perkin–Elmer LS-55 spectrofluorimeter (with the excitation and emission slits fixed at 5 and 7.5 nm, respectively), and all spectra were corrected for the instrument response function. A standard solid sample holder was used for mounting of solid sample and an appropriate attenuator was used to avoid saturation of signal.

2.2. *Synthesis of dihalocadmium(II) compounds (1–12)*

$[Cd(X_2)(L)]$ (**4**, **10**), $[Cd(X_2)(L)(DMSO)]$ (**9**), $[Cd(X_2)(L)]_2$ (**1–3**, **5**, **7**, **8**, **11**, and **12**), and $[Cd(Cl_2)_2(L)]_n$ (**6**)

The methods employed for the preparation of the dihalocadmium(II) compounds (**1–12**) are very similar, so that the preparation of the dibromide derivative (**1**) is given in detail as a representative example.

2.2.1. Synthesis of $[Cd(Br)_2(L^1)]_2$ (1). To a solution of pyridine-2-carboxaldehyde (0.172 g, 1.60 mM) in ethanol (5 mL) was added a solution of aniline (0.15 g, 1.61 mM) in ethanol (5 mL). The mixture was stirred at ambient temperature for 30 min. To this reaction mixture, $CdBr_2$ (0.44 g, 1.61 mM) in methanol (20 mL) was added dropwise under stirring which resulted in the immediate formation of a yellow precipitate. Stirring was continued for 3 h after which the mixture was filtered. The residue was washed with methanol (3 × 5 mL) and dried *in vacuo*. The dried solid was dissolved by boiling in acetonitrile (60 mL) and filtered while hot. The filtrate, upon cooling to room temperature, afforded a yellow crystalline material. Yield 0.30 g (39%). M.p.: 258–260 °C. Found: C, 31.68; H, 2.32; N, 6.06%. Calcd for $C_{24}H_{20}Br_4Cd_2N_4$: C, 31.72; H, 2.22; N, 6.16%. Λ_m (CH_3CN): 3.3 $\Omega^{-1}cm^2$ M^{-1}. IR (cm^{-1}): 1627 ν_{asym}(C(H)=N); 1591, 1492, 1436 ν(C=N)py. ^{1}H-NMR (DMSO-d_6): δ 9.15 [d, J = 4 Hz, 1H, H-3′], 8.66 [s, 1H, H-7], 8.14 [t, J = 8.0 Hz, 1H, H-5′], 7.93 [d, J = 8.0 Hz, 1H, H-6′], 7.77 [t, J = 6.4 Hz, 1H, H-4′], 7.43 [d, J = 8.0 Hz, 2H, H-3,5], 7.30 [m, 3H, H-2,4,6] ppm. The atom numbering scheme employed is shown in chart 1.

2.2.2. Synthesis of $[Cd(Br)_2(L^2)]_2{\cdot}C_6H_6$ (2). A similar synthetic procedure as that used for **1** was used except that aniline was replaced by *o*-toluidine, giving pale-yellow crystals of the benzene monosolvate from acetonitrile/benzene (*v*/*v*, 6 : 1) solution. Yield 61%. M.p.: 172–175 °C. Found: C, 37.75; H, 3.10; N, 5.27%. Calcd for $C_{32}H_{30}Br_4Cd_2N_4$: C, 37.86; H, 2.97; N, 5.52%. Λ_m (CH_3CN): 3.5 $\Omega^{-1}cm^2$ M^{-1}. IR (cm^{-1}): 1639 ν_{asym}(C(H)=N); 1600, 1500, 1447 ν(C=N)py. ^{1}H-NMR (DMSO-d_6): δ 8.97 [d, J = 4.0 Hz, 1H, H-3′], 8.57 [s, 1H, H-7], 8.16 [t, J = 8.0 Hz, 1H, H-6′], 8.01 [d, J = 8.0 Hz, 1H, H-5′], 7.75 [t, J = 6.4 Hz, 1H, H-4′], 7.21 [m, 3H, H-3,5,6], 7.01 [t, J = 6.4 Hz, 1H, H-4], 2.32 [s, 3H, CH_3] ppm.

2.2.3. Synthesis of $[Cd(Br)_2(L^3)]_2$ (3). A similar synthetic procedure as that used for **1** was used except that aniline was replaced by *p*-toluidine, giving pale-yellow crystals from

acetonitrile solution. Yield 55%. M.p.: 279–280 °C. Found: C, 33.02; H, 2.66; N, 6.19%. Calcd for $C_{26}H_{24}Br_4Cd_2N_4$: C, 33.37; H, 2.58; N, 5.98%. Λ_m (CH_3CN): 2.0 $\Omega^{-1}cm^2$ M^{-1}. IR (cm^{-1}): 1626 ν_{asym}(C(H)=N); 1589, 1506, 1439 ν(C=N)py. ^{1}H-NMR (DMSO-d_6): δ 9.05 [d, J = 4.0 Hz, 1H, H-3′], 8.74 [s, 1H, H-7], 8.15 [t, J = 8.0 Hz, 1H, H-6′], 8.00 [d, J = 8.0 Hz, 1H, H-5′], 7.77 [t, J = 6.4 Hz, 1H, H-4′], 7.38 [d, J = 8.0 Hz, 2H, H-3,5], 7.16 [d, J = 8.0 Hz, 2H, H-2,6], 2.35 [s, 3H, CH_3] ppm.

2.2.4. Synthesis of $[Cd(Br)_2(L^4)]$ (4). A similar synthetic procedure as that used for **1** was used except that aniline was replaced by *o*-anisidine, giving pale-yellow crystals from acetonitrile/dimethylsulfoxide (*v*/*v*, 6 : 1) solution. Yield 49%. M.p.: 265–266 °C. Found: C, 32.44; H, 2.50; N, 5.66%. Calcd for $C_{13}H_{12}Br_2CdN_2O$: C, 32.26; H, 2.50; N, 5.79%. Λ_m (CH_3CN): 1.3 $\Omega^{-1}cm^2$ M^{-1}. IR (cm^{-1}): 1623 ν_{asym}(C(H)=N); 1590, 1495, 1439 ν(C=N)py. ^{1}H-NMR (DMSO-d_6): δ 9.02 [s, 1H, H-7], 8.80 [d, 1H, H-3′], 8.13 [t, 1H, H-6′], 8.00 [d, 1H, H-5′], 7.73 [t, 1H, H-4′], 7.44 [d, 1H, H-6], 7.29 [t, 1H, H-4], 6.96 [m, 2H, H-3,5], 3.81 [s, 3H, OCH_3] ppm.

2.2.5. Synthesis of $[Cd(Br)_2(L^5)]_2 \cdot 2CH_3CN$ (5). A similar synthetic procedure as that used for **1** was used except that aniline was replaced by *p*-anisidine, giving-yellow crystals of the acetonitrile disolvate from acetonitrile/dimethylsulfoxide (*v*/*v*, 6 : 1) solution. Yield 55%. M.p.: 255–258 °C. Found: C, 34.05; H, 2.52; N, 7.50%. Calcd for $C_{30}H_{30}Br_4Cd_2N_6O_2$: C, 34.28; H, 2.87; N, 7.99%. Λ_m (CH_3CN): 1.5 $\Omega^{-1}cm^2$ M^{-1}. IR (cm^{-1}): 1624 ν_{asym}(C(H)=N); 1596, 1507, 1441 ν(C=N)py. ^{1}H-NMR (DMSO-d_6): δ 9.14 [d, J = 4.0 Hz, 1H, H-3′], 8.61 [s, 1H, H-7], 8.11 [t, J = 8.0 Hz, 1H, H-6′], 7.85 [d, J = 8.0 Hz, 1H, H-5′], 7.72 [t, J = 6.4 Hz, 1H, H-4′], 7.53 [d, br, 2H, H-3,5], 6.83 [d, J = 8.0 Hz, 2H, H-2,6], 3.80 [s, 3H, OCH_3] ppm.

2.2.6. Synthesis of $[Cd(Cl)_2(L^2)]$ (6). A similar synthetic procedure as that used for **1** was used except that $CdBr_2$ and aniline were replaced by $CdCl_2$ and *o*-toluidine, respectively, giving pale-yellow crystals from acetonitrile. Yield 53%. M.p.: 242–245 °C. Found: C, 41.34; H, 3.22; N, 7.30%. Calcd for $C_{13}H_{12}CdCl_2N_2$: C, 41.14; H, 3.19; N, 7.38%. Λ_m (CH_3CN): 3.3 $\Omega^{-1}cm^2$ M^{-1}. IR (cm^{-1}): 1639 ν_{asym}(C(H)=N); 1593, 1487, 1440 ν(C=N)py. ^{1}H-NMR (DMSO-d_6): δ 8.94 [d, J = 4.0 Hz, 1H, H-3′], 8.57 [s, 1H, H-7], 8.14 [t, J = 8.0 Hz, 1H, H-6′], 8.02 [d, J = 8.0 Hz, 1H, H-5′], 7.71 [t, 6.4 1H, H-4′], 7.19 [m, 3H, H-3,5,6], 6.99 [t, J = 6.4 Hz, 1H, H-4], 2.30 [s, 3H, CH_3] ppm.

2.2.7. Synthesis of $[Cd(Cl)_2(L^6)]_2$ (7). A similar synthetic procedure as that used for **1** was used except that $CdBr_2$ and aniline were replaced by $CdCl_2$ and *p*-chloroaniline, respectively, giving pale-yellow crystals from acetonitile. Yield 41%. M.p.: 288–290 °C. Found: C, 36.33; H, 2.20; N, 6.89%. Calcd for $C_{24}H_{18}Cd_2Cl_6N_4$: C, 36.03; H, 2.26; N, 7.00%. Λ_m (CH_3CN): 3.0 $\Omega^{-1}cm^2$ M^{-1}. IR (cm^{-1}): 1624 ν_{asym}(C(H)=N); 1597, 1507, 1441 ν(C=N)py. ^{1}H-NMR (DMSO-d_6): δ 9.01 [d, J = 4.0 Hz, 1H, H-3′], 8.80 [s, 1H, H-7], 8.16 [t, J = 8.0 Hz, 1H, H-6′], 8.08 [d, J = 8.0 Hz, 1H, H-5′], 7.74 [t, J = 6.4 Hz, 1H, H-4′], 7.56 [d, J = 8.0 Hz, 2H, H-3,5], 7.40 [d, J = 8.0 Hz, 2H, H-2,6] ppm.

2.2.8. Synthesis of $[Cd(I)_2(L^3)]_2$ (8). A similar synthetic procedure as that used for **1** was used except that $CdBr_2$ and aniline were replaced by CdI_2 and *p*-toluidine, respectively, giving pale-yellow crystals from acetonitile. Yield 35%. M.p.: 235–238 °C. Found: C, 27.48; H, 2.44; N, 5.18%. Calcd for $C_{26}H_{24}Cd_2I_4N_4$: C, 27.69; H, 2.14; N, 4.96%. Λ_m (CH_3CN): 2.0 $\Omega^{-1}cm^2$ M^{-1}. IR (cm^{-1}): 1635 ν_{asym}(C(H)=N); 1597, 1488, 1444 ν(C=N)py. ^{1}H-NMR (DMSO-d_6): δ 8.91 [d, 1H, H-3′], 8.56 [s, 1H, H-7], 8.13 [t, 1H, H-6′], 7.94 [d, 1H, H-5′], 7.77 [t, 1H, H-4′], 7.00 [d, 2H, H-3,5], 6.88 [d, J = 8.0 Hz, 2H, H-2,6], 2.27 [s, 3H, CH_3] ppm.

2.2.9. Synthesis of $[Cd(I)_2(L^3)(DMSO)]$ (9). A similar synthetic procedure as that used for **1** was used except that $CdBr_2$ and aniline were replaced by CdI_2 and *p*-toluidine, respectively, giving pale-yellow crystals from acetonitile/dimethylsulfoxide (*v/v*, 6 : 1) solution. Yield 35%. M.p.: 253–255 °C. Found: C, 28.18; H, 2.99; N, 4.26%. Calcd for $C_{15}H_{18}CdI_2N_2OS$: C, 28.06; H, 2.82; N, 4.36%. Λ_m (CH_3CN): 2.0 $\Omega^{-1}cm^2$ M^{-1}. IR (cm^{-1}): 1624 ν_{asym}(C(H)=N); 1596, 1507, 1441 ν(C=N)py; 1023 ν(S=O). ^{1}H-NMR in DMSO-d_6 displayed signals identical to those observed for its uncoordinated DMSO compound **8** and were indistinguishable.

2.2.10. Synthesis of $[Cd(I)_2(L^4)]$ (10). A similar synthetic procedure as that used for **1** was used except that $CdBr_2$ and aniline were replaced by CdI_2 and *o*-anisidine, respectively, giving pale-yellow crystals from acetonitile/dimethylsulfoxide (*v/v*, 6 : 1) solution. Yield 43%. M.p.: 265–266 °C. Found: C, 27.19; H, 2.29; N, 5.04%. Calcd for $C_{13}H_{12}CdI_2N_2O$: C, 26.99; H, 2.09; N, 4.84%. Λ_m (CH_3CN): 1.0 $\Omega^{-1}cm^2$ M^{-1}. IR (cm^{-1}): 1618 ν_{asym}(C(H)=N); 1589, 1495, 1438 ν(C=N)py. ^{1}H-NMR (DMSO-d_6): δ 9.08 [s, 1H, H-7], 8.88 [d, J = 4.0 Hz, 1H, H-3′], 8.21 [t, J = 8.0 Hz, 1H, H-6′], 8.09 [d, J = 8.0 Hz, 1H, H-5′], 7.81 [t, J = 6.4 Hz, 1H, H-4′], 7.44 [d, J = 6.4 Hz, 1H, H-6], 7.36 [t, J = 8.0 Hz, 1H, H-4], 7.03 [m, 2H, H-3,5], 3.86 [s, 3H, OCH_3] ppm.

2.2.11. Synthesis of $[Cd(I)_2(L^5)]_2$ (11). A similar synthetic procedure as that used for **1** was used except that $CdBr_2$ and aniline were replaced by CdI_2 and *p*-anisidine, respectively, giving pale-yellow crystals from acetonitile/dimethylsulfoxide (*v/v*, 6 : 1) solution. Yield 41%. M.p.: 202–205 °C. Found: C, 26.85; H, 2.22; N, 4.74%. Calcd for $C_{26}H_{24}Cd_2I_4N_4O_2$: C, 26.99; H, 2.09; N, 4.84%. Λ_m (CH_3CN): 2.0 $\Omega^{-1}cm^2$ M^{-1}. IR (cm^{-1}): 1624 ν_{asym}(C(H)=N); 1596, 1507, 1441 ν(C=N)py. ^{1}H-NMR (DMSO-d_6): δ 9.14 [d, J = 4.0 Hz, 1H, H-3′], 8.61 [s, 1H, H-7], 8.12 [t, J = 8.0 Hz, 1H, H-6′], 7.86 [d, J = 8.0 Hz, 1H, H-5′], 7.75 [t, J = 6.4 Hz, 1H, H-4′], 7.49 [d, br, 2H, H-3,5], 6.84 [d, J = 8.0 Hz, 2H, H-2,6], 3.80 [s, 3H, OCH_3] ppm.

2.2.12. Synthesis of $[Cd(I)_2(L^6)]_2$ (12). A similar synthetic procedure as that used for **1** was used except that $CdBr_2$ and aniline were replaced by CdI_2 and *p*-chloroaniline, respectively, giving pale-yellow crystals from acetonitile solution. Yield 47%. M.p.: 238–240 °C. Found: C, 24.80; H, 1.66; N, 4.80%. Calcd for $C_{24}H_{18}Cd_2Cl_2I_4N_4$: C, 24.68; H, 1.55; N, 4.79%. Λ_m (CH_3CN): 2.0 $\Omega^{-1}cm^2$ M^{-1}. IR (cm^{-1}): 1625 ν_{asym}(C(H)=N); 1591, 1489, 1440 ν(C=N)py. ^{1}H-NMR (DMSO-d_6): δ 9.12 [d, J = 4.0 Hz, 1H, H-3′], 8.66 [s, 1H, H-7], 8.12

Table 1. Crystal data and refinement details for **1–12**.

	1	**2**	**3**	**4**	**5**	**6**
Empirical formula	$C_{24}H_{20}Br_4Cd_2N_4$	$C_{26}H_{24}Br_4Cd_2N_4.C_6H_6$	$C_{26}H_{24}Br_4Cd_2N_4$	$C_{13}H_{12}Br_2CdN_2O$	$C_{26}H_{24}Br_4Cd_2N_4O_2.2C_2H_3N$	$C_{13}H_{12}CdCl_2N_2$
Formula weight	908.88	1015.04	936.93	484.47	1051.04	379.56
Crystal size (mm)	0.02 × 0.10 × 0.20	0.25 × 0.30 × 0.35	0.05 × 0.20 × 0.20	0.20 × 0.20 × 0.20	0.10 × 0.15 × 0.35	0.10 × 0.15 × 0.30
Crystal system	Triclinic	Triclinic	Monoclinic	Monoclinic	Triclinic	Triclinic
Space group	$P\bar{1}$	$P\bar{1}$	$P2_1/n$	Pc	$P\bar{1}$	$P\bar{1}$
a (Å)	8.2294(6)	7.6933(3)	7.6995(3)	8.2524(6)	9.4583(4)	7.0360(4)
b (Å)	8.6786(5)	9.9307(4)	15.8390(5)	12.1119(7)	10.0120(5)	9.6569(5)
c (Å)	10.0140(6)	11.6490(5)	12.2233(5)	8.1310(7)	10.2342(4)	10.5218(5)
α (°)	107.055(6)	108.351(4)	90	90	88.542(4)	98.100(4)
β (°)	102.277(6)	91.100(4)	98.312(4)	114.761(10)	66.009(4)	104.740(4)
γ (°)	98.834(6)	94.630(4)	90	90	77.901(4)	94.793(4)
V (Å^3)	650.01(7)	841.03(6)	1475.00(10)	737.99(9)	863.81(7)	679.14(6)
Z	1	1	2	2	1	2
D_x (g cm^{-3})	2.322	2.004	2.110	2.180	2.020	1.856
μ (mm^{-1})	7.804	6.043	6.882	6.886	5.893	1.983
θ Range (°)	2.9–27.6	2.4–27.6	2.6–27.6	2.7–27.6	2.4–27.6	2.7–27.6
Reflections measured	10,687	12,101	9982	4918	12,424	9821
Independent reflections; R_{int}	3006; 0.071	3857; 0.041	3390; 0.048	2481; 0.043	3988; 0.042	3147; 0.045
Reflections with $I > 2\sigma(I)$	2318	3458	2852	2303	3509	2769
Number of parameters	154	191	164	173	200	164
$R(F)$ [$I > 2\sigma(I)$ reflns]	0.038	0.024	0.028	0.033	0.026	0.024
a, b in weighting scheme	0.029, 0	0.015, 0	0.016, 0	0.055, 0	0.024, 0	0.019, 0
$wR(F^2)$ (all data)	0.085	0.048	0.055	0.086	0.060	0.052
GOF(F^2)	1.04	1.03	1.02	0.99	1.03	1.01
$\Delta\rho_{max,\ min}$ (e Å^{-3})	1.35, −1.21	0.84, −0.60	0.57, −0.68	0.95, −1.08	0.48, −0.71	0.81, −0.71

(*Continued*)

Table 1. (*Continued*)

	7	**8**	**9**	**10**	**11**	**12**
Empirical formula	$C_{24}H_{18}Cd_2Cl_6N_4$	$C_{26}H_{24}Cd_2I_4N_4$	$C_{15}H_{18}CdI_2N_2OS$	$C_{13}H_{12}CdI_2N_2O$	$C_{26}H_{24}Cd_2I_4N_4O_2$	$C_{24}H_{18}Cd_2Cl_2I_4N_4$
Formula weight	799.92	1124.90	640.57	578.45	1156.89	1165.72
Crystal size (mm)	0.05 × 0.10 × 0.25	0.05 × 0.10 × 0.20	0.05 × 0.20 × 0.20	0.05 × 0.15 × 0.25	0.15 × 0.20 × 0.25	0.10 × 0.20 × 0.30
Crystal system	Monoclinic	Triclinic	Monoclinic	Monoclinic	Monoclinic	Monoclinic
Space group	$P2_1/n$	$P\bar{1}$	$P2_1$	Pc	$P2/c$	$P2_1/n$
a (Å)	7.5362(7)	7.9188(4)	7.8278(4)	8.3262(7)	7.7394(3)	7.9625(2)
b (Å)	14.8258(10)	9.3567(5)	15.5331(8)	12.1278(7)	9.9390(3)	17.0367(5)
c (Å)	12.4516(9)	10.9692(7)	8.1860(4)	8.6962(6)	20.5832(7)	11.5052(3)
α (°)	90	103.012(5)	90	90	90	90
β (°)	95.830(8)	101.383(5)	102.946(5)	114.234(9)	96.714(3)	96.321(3)
γ (°)	90	100.198(5)	90	90	90	90
V (Å^3)	1384.02(19)	755.14(7)	970.04(8)	800.75(10)	1572.44(9)	1551.25(7)
Z	2	1	2	2	2	2
D_x (g cm^{-3})	1.919	2.474	2.193	2.399	2.443	2.496
μ (mm^{-1})	2.138	5.518	4.418	5.212	5.309	5.544
θ Range (°)	2.8–27.6	3.1–26.4	3.7–27.6	2.7–27.6	2.3–27.6	2.8–27.6
Reflections measured	9312	9896	8445	5352	10,312	10,434
Independent reflections; R_{int}	3199; 0.071	3079; 0.053	4240; 0.034	2739; 0.035	3620; 0.027	3574; 0.026
Reflections with $I > 2\sigma(I)$	2268	2530	4087	2602	3296	3255
Number of parameters	163	164	202	173	172	164
$R(F)$ [$I > 2\sigma(I)$ reflns]	0.053	0.032	0.029	0.030	0.025	0.022
a, b in weighting scheme	0.051, 0	0.021, 0	0.024, 0	0.044, 0	0.030, 0.103	0.026, 0
$wR(F^2)$ (all data)	0.135	0.065	0.060	0.074	0.063	0.051
GOF(F^2)	1.07	0.99	1.00	0.99	1.10	1.01
$\Delta\rho_{max,\ min}$ (e Å^{-3})	2.45−1.15	0.86−0.98	0.60−0.95	0.69−1.31	0.61−1.55	0.75−0.67

[t, J = 8.0 Hz, 1H, H-6′], 7.95 [d, J = 8.0 Hz, 1H, H-5′], 7.78 [t, J = 6.4 Hz, 1H, H-4′], 7.36 [d, J = 8.0 Hz, 2H, H-3,5], 7.26 [d, J = 8.0 Hz, 2H, H-2,6] ppm.

2.3. *X-ray crystallography*

Yellow/pale-yellow crystals of the compounds suitable for X-ray crystal structure determination were obtained from acetonitrile/chloroform (*v*/*v*, 3 : 1) (**1**, **3**, **6–8,** and **12**), or acetonitrile/benzene/chloroform (*v*/*v*, 3 : 1 : 1) (**2**) or acetonitrile/dimethylsulfoxide (*v*/*v*, 6 : 1) (**4**, **5**, and **9–11**) by slow evaporation of the solvent at room temperature. The intensity measurements were made at 100 K on an Agilent Supernova dual diffractometer with an Atlas (Mo) detector (ω scan technique) using graphite-monochromated Mo Kα radiation [48]. The structures were solved by direct methods (SHELXS97 [49] through the WinGX Interface [50]) and refined (anisotropic displacement parameters, H atoms in the riding model approximation and a weighting scheme of the form $w = 1/[\sigma^2(F_o^2) + aP^2 + bP]$ where $P = (F_o^2 + 2F_c^2)/3)$ with SHELXL97 on F^2 [49]. The absolute structures of **4**, **9**, and **10** were determined on the basis of differences in Friedel pairs included in the respective data-sets. When present, residual electron density peaks >1.0 eÅ^{-3} were located near the Cd atom and/or near the halide (Br and I). The data collection and refinement parameters are given in table 1, and views of the molecular structures are shown in figures 4–8, drawn at the 50% probability level with ORTEP-3 for Windows [50]; the crystal packing analysis was conducted with the aid of PLATON [51] and diagrams were drawn with DIAMOND [52].

3. Results and discussion

3.1. *Synthesis*

To understand the structural trends of cadmium dihalide complexes with L, a series of 12 new compounds, **1–12** (chart 1), were synthesized. Synthesis was achieved by template reactions between pyridine-2-carboxaldehyde, aniline, or derivatives and cadmium dihalides in a mole ratio 1 : 1 : 1, according to a route described for cognate mercury(II) compounds [47]. All cadmium compounds of the present investigation are insoluble in the reaction medium, but can be recrystallized using a large volume of acetonitrile or combination of acetonitrile and DMSO or only in DMSO. Molar conductivity measurements indicated that **1–12** are non-electrolytes. These results along with elemental analysis show that the M : X ratio present in the original salts is preserved in the new compounds and that the L^1–L^6 ligands are present in neutral forms. Compounds **1–12** are all air-stable. The results of the chemical and spectroscopic analyses are consistent with the crystal structure determinations of **1–12** (see below).

3.2. *Spectroscopic characterization*

The infrared spectra of **1–12** are very similar, and the assignments of selected diagnostic bands are given in the *Experimental section*. The compounds display a moderately intense IR band at 1618–1640 cm^{-1}, which is assigned to the ν_{asym}(C(H)=N) stretch of the coordinated Schiff base ligands [47, 53]. In addition, well-resolved bands of variable intensity

observed at 1600–1580, 1490–1475, and 1450–1435 cm^{-1} are assigned to the coordinated pyridyl ring [53–55]. Compound **9**, in addition to usual ν(C(H)=N) and ν(C=N)py bands, displayed a very strong band at 1023 cm^{-1}, which is attributed to ν(S=O) of the coordinated DMSO molecule. This value is 35 cm^{-1} lower than that reported for free DMSO (1055 cm^{-1}) and is thus indicative of terminal (end-on) *O*-coordination. It should be noted that for *S*-bonded DMSO, an increase in frequency is expected [56, 57]. The ^{1}H NMR spectra were recorded in DMSO-d_6 solution which displayed the expected signals and integration values. In general, the signals were broad. However, coupling constants could be determined in many cases, as detailed in the *Experimental section*; except for **4** and **8** owing to complicated splitting yet the multiplicity patterns could be delineated. Compounds **2** and **5** should also display ^{1}H NMR signals due to benzene and acetonitrile solvates but these were obscured in the NMR spectra in DMSO-d_6 solvent.

Table 2 summarizes the solution UV–vis and fluorescence properties of **1–12**. The absorption spectra of all compounds were recorded in the range 300–450 nm in acetonitrile solutions at concentrations of ~10^{-5} M. The experimental absorption spectra comprise two overlapping bands at 325–360 nm (figure S1 Supplemental data for this article can be accessed http://dx.doi.org/10.1080/00958972.2013.864393); data for the free ligands are not available for comparison as free ligands could not be isolated in pure forms. It is well known that cadmium(II) compounds show excellent luminescence properties [58] and accordingly, the photoluminescence properties of **1–12** in acetonitrile solution were investigated. Generally, at room temperature, broad fluorescent emission bands at λ_{max} = 405 nm along with a shoulder in the range ~440–455 nm were observed. The exceptional spectra were for each of **4** and **10**, i.e. the *o*-methoxy derivatives, which appeared at higher wavelengths, i.e. ~495 nm, when they are excited at their respective absorption maxima (figure S2). These emissions could not be assigned as metal-to-ligand charge transfer (MLCT) or ligand-to-metal charge transfer (LMCT) as the cadmium(II) ion, with a d^{10} configuration, is not easy to oxidize or reduce [59]. The emissions are therefore attributed to the intraligand (IL) (π–π^*) fluorescent emission. Recently, a molecule containing a related ligand backbone as in L^1–L^6, i.e. (*E*)-4-((pyridin-2-ylmethylidene)amino)phenol was synthesized and found

Table 2. Photophysical data for **1–12** recorded in acetonitrile solution and in the solid-state.

		Photoluminescence data		
		Solution-state		Solid-state
Compounds	Electronic spectroscopic data λ_{max} (nm); (ε[M^{-1}])	λ_{em} (nm)[a]	ϕ_F	λ_{em} (nm)[a]
1	324 (12,272)	403, 441	0.06	425, 490
2	334 (9605)	404, 446	0.04	452, 485
3	341 (13,320)	404, 442	0.07	434, 484
4	310 (12,500) 365 (14,717)	404, 497	0.04	491
5	363 (14,637)	404, 446	0.03	498
6	331 (7904)	403, 443	0.05	414, 487
7	334 (11,133)	404, 439	0.03	437, 482
8	334 (15,896)	406, 439	0.05	443, 482
9	334 (15,397)	403, 447	0.02	435, 487
10	315 (15,291) 367 (17,815)	406, 496	0.11	482, 518
11	365 (17,718)	406, 454	0.03	517
12	326 (15,920)	403, 442	0.01	451, 480

[a]The high energy wavelength emission appears as a shoulder in all cases.

to be non-emissive in solution and in the solid state, even at 77 K [60]. However, such observations should not be generalized for the emission properties of L. Overall, the present investigation show very low fluorescent quantum yields (table 2), indicating that the cadmium(II) compounds are weak emitters at room temperature. The small variations in photoluminescence across the series may be attributed to differences in the constitution of L, anions and/or their local coordination environment. The solid-state fluorescence spectra for all the assayed compounds at room temperature displayed rather a broad emission band at λ_{max} ~445 nm along with a shoulder in the range ~475–490 nm akin to that observed in solution, except for those with –OMe substituent at Y or Z position (*cf.* Chart 1; compounds **4**, **5**, **10**, and **11**). Interestingly, **4**, **5**, **10**, and **11** show a single band emission which is appreciably red-shifted with respect to the other investigated compounds (*cf.* figure S3). Similar behavior was noted in the spectra of acetonitrile solution and such shift could be attributed to extra stabilization by the –OMe substitution. The presence of –OMe group at the *ortho*-position in **4** and **10** hindered flexible motion at the connecting N-center through crowding and thereby increase fluorescence by resisting non-radiative channels which is usually active through flexible modes in solution phase. However, such possibility is absent when –OMe group is at the *para*-position and hence the observed fluorescence intensities of the red-shifted band of **5** and **11** are low in solution. On the other hand, in the solid matrix such non-radiative channels through flexible modes are absent by rigid solid matrix and hence the fluorescence intensity of the red-shifted band for all the compounds (**4**, **5**, **10** and **11**) is high. Such observation clearly suggests that in those compounds there is an intraligand charge transfer which stabilizes the whole system and thus accounts for the observed red shift [61, 62].

3.3. *Molecular structures*

The crystal and molecular structures of **1–12** have been determined; crystal data and selected geometric parameters are shown in tables 1 and 3, respectively. The structures of the $CdBr_2$ series (**1–5**) are discussed first and then related to their $CdCl_2$ (**6**, **7**) and CdI_2 (**8–12**) analogs. The structural motifs range from mononuclear to binuclear and polymeric with variations related to the Lewis acidity of the cadmium center, coordination of additional donor atoms on the L^n ligands, chelating ability of L^n, and due to interaction with solvent molecules.

The molecular structure of $[Cd(Br)_2(L^1)]_2$ (**1**) is shown in figure 1 and serves as the prototype for the majority of structures described herein. The binuclear molecule is generated by the application of a center of inversion and features two cadmium ions bridged in an asymmetric manner by two bromo ligands. As anticipated, the Cd–Br (bridging) distances are longer than the terminal Cd–Br bond length. L chelates through the nitrogen atoms, consistent with an earlier analysis [47]; the Cd–N(pyridyl) bond length is significantly shorter than the Cd–N(imino) bond length, a trend that holds true of all binuclear molecules in the present study. The ligand backbone is planar as seen in the values of the N1–C5–C6–N2 torsion angles and this planarity is sometimes extended to include the pendant aryl ring (table 3). The resultant five-membered CdN_2C_2 chelate ring is planar with the root-mean-square (r.m.s.) deviation of the fitted atoms being 0.049 Å. The Br_3N_2 donor set defines a coordination geometry approaching square pyramidal as quantified by the value of $\tau = 0.27$ which compares to the τ values of 0.0 and 1.0 for ideal square pyramidal and trigonal bipyramidal geometries, respectively [63]. A partial explanation for the distortion is traced

Table 3. Selected geometric parameters (Å, °) for **1–12**.

Compound	**1** (X = Br)	**2** (X = Br)	**3** (X = Br)	**4** (X = Br)	**5** (X = Br)	**6** (X = Cl)[a]
Cd–X1	2.6869(7)	2.6330(3)	2.6376(4)	2.5369(9)	2.6555(4)	2.5787(6)
Cd–X1^{i}	2.7689(7)	2.8076(3)	2.8021(4)	–	2.8005(4)	2.6547(6)
Cd–X2	2.5388(7)	2.5571(3)	2.5486(4)	2.5397(9)	2.5578(4)	2.5163(6)
Cd–N1	2.312(4)	2.301(2)	2.287(3)	2.324(5)	2.287(2)	2.351(2)
Cd–N2	2.405(4)	2.412(2	2.413(2)	2.321(6)	2.408(2)	2.4260(19)
Cd–Y	–	–	–	2.504(4) (O1)	–	2.6917(6) (Cl2^{ii})
N1–Cd–N2	71.92(15)	72.03(7)	72.37(9)	71.71(18)	72.36(8)	69.94(6)
X1–Cd–X2	109.69(2)	130.987(12)	127.487(15)	116.45(3)	117.848(13)	103.15(2)
X1–Cd–X1^{i}	86.40(2)	85.124(10)	87.016(12)	–	86.337(11)	85.563(17)
X2–Cd–X1^{i}	105.13(2)	97.875(10)	97.708(13)	–	99.436(11)	96.930(19)
X1–Cd–N1	131.83(11)	128.92(5)	116.33(7)	102.78(15)	118.27(6)	92.71(5)
X1^{i}–Cd–N2	148.24(10)	151.86(5)	158.92(6)	–	159.39(6)	80.89(5)
N1–Cd–Y	–	–	–	135.52(18) (O1)	–	80.38(5) (Cl2^{ii})
Cd–X1–Cd^{i}	93.60(2)	94.876(10)	92.984(12)	–	93.663(11)	94.437(17)
N2–C6	1.288(7)	1.286(3)	1.280(4)	1.277(8)	1.279(4)	1.264(3)
N1–C5–C6–N2	4.9(8)	−6.9(3)	4.9(5)	−0.9(10)	2.0(4)	9.6(3)
C6–N2–C7–C8	−16.9(8)	−40.9(3)	−13.0(5)	13.1(11)	−7.6(4)	−128.1(3)
Symmetry operation:	$2-x, 1-y, 1-z$	$1-x, 1-y, 1-z$	$1-x, 1-y, 1-z$	–	$1-x, 1-y, 1-z$	$1-x, 1-y, 1-z$

Compound	**7** (X = Cl)	**8** (X = I)	**9** (X = I)	**10** (X = I)	**11** (X = I)	**12** (X = I)
Cd–X1	2.5122(15)	2.8611(5)	2.7636(5)	2.7182(7)	2.8009(3)	2.8340(3)
Cd–X1^{i}	2.6505(15)	2.9865(6)	–	–	3.0513(4)	3.0021(3)
Cd–X2	2.4119(16)	2.7295(6)	2.7541(5)	2.7090(7)	2.7416(3)	2.7206(3)
Cd–N1	2.277(5)	2.338(4)	2.303(4)	2.319(6)	2.305(3)	2.305(2)
Cd–N2	2.388(5)	2.428(4)	2.440(4)	2.313(6)	2.438(3)	2.431(2)
Cd–Y	–	–	2.366(4) (O1)	2.534(5) (O1)	–	–
N1–Cd–N2	72.10(17)	71.00(15)	71.60(15)	71.4(2)	71.33(10)	71.68(8)
X1–Cd–X2	123.47(6)	113.360(18)	120.089(16)	117.32(2)	122.881(12)	125.655(10)
X1–Cd–X1^{i}	88.27(5)	87.519(16)	–	–	88.887(10)	86.383(8)
X2–Cd–X1^{i}	94.70(5)	100.769(16)	–	–	96.992(10)	102.125(9)
X1–Cd–N1	111.21(13)	121.49(11)	114.51(11)	113.54(16)	111.89(7)	117.96(6)
X1^{i}–Cd–N2	160.33(13)	152.60(11)	–	–	162.32(7)	154.36(6)
N1–Cd–Y	–	–	82.25(14)	134.1(2)	–	–
Cd–X1–Cd^{i}	91.73(5)	87.519(16)	–	–	84.313(10)	86.383(8)
N2–C6	1.274(8)	1.269(7)	1.278(6)	1.283(9)	1.278(4)	1.277(4)
N1–C5–C6–N2	4.3(9)	−3.0(8)	−1.4(8)	1.1(10)	−0.8(5)	−1.3(4)
C6–N2–C7–C8	−21.9(9)	11.8(8)	3.7(8)	−13.1(11)	5.3(5)	3.4(4)
Symmetry operation *i*:	$1-x, 1-y, 1-z$	$-x, 1-y, 1-z$	–	–	$1-x, y, ½-z$	$1-x, 1-y, 1-z$

[a]Symmetry operation *ii*: $2-x, 1-y, 1-z$; additional angles: Cl1^{i}–Cd–Cl2^{ii} = 178.214(18), Cl1–Cd–N2 = 155.49(6), Cl2–Cd–N1 = 157.47(5), Cd–Cl2–Cd^{ii} = 97.058(19)°.

to the restricted bite angle of L. Allowing for chemical differences, very similar binuclear molecular structures are found for $[Cd(Br)_2(L^2)]_2{\cdot}C_6H_6$ (**2**) and $[Cd(Br)_2(L^3)]_2$ (**3**), where each of L^2 and L^3 carries a methyl substituent in the aryl ring (figure S4).

Each binuclear molecule of **2** and **3** is located about a center of inversion. A solvent benzene molecule, also disposed about a center of inversion, crystallized with **2** so that the overall stoichiometry is $[Cd(Br)_2(L^2)]_2{\cdot}C_6H_6$. The τ values of 0.35 and 0.52, respectively, are closer to trigonal bipyramidal than observed in **1**. The Cd–Br bridges are less symmetric in these structures with Δ(Cd–Br) = difference in the Cd–Br(bridging) distances = 0.175 and 0.165 Å, respectively, compared with Δ(Cd–Br) = 0.082 Å in **1**. The greater asymmetry in each of **2** and **3** arises as a result of the contraction of the shorter Cd–Br bridging distance and elongation of the longer Cd–Br(bridge) distance; there is also an elongation of the terminal Cd–Br bond length. These observations are correlated with the better

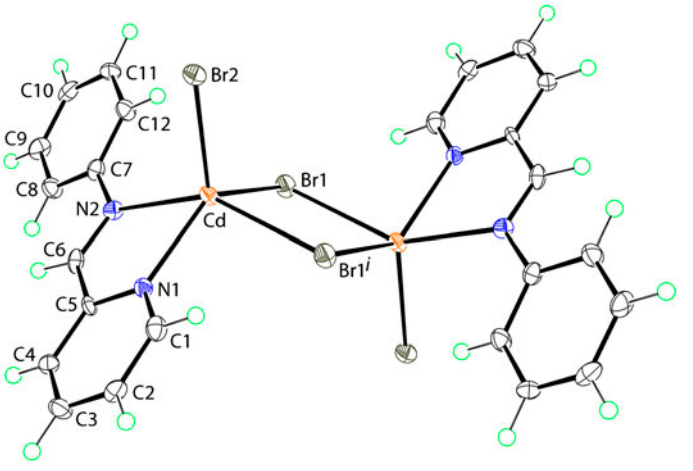

Figure 1. Molecular structure of binuclear $[Cd(Br)_2(L^1)]_2$ (**1**). Unlabeled atoms are related by the symmetry operation $2-x, 1-y, 1-z$. Allowing for differences in halide and substituents in L, the molecular structures of $[Cd(Br)_2(L^2)]_2{\cdot}C_6H_6$ (**2**), $[Cd(Br)_2(L^3)]_2$ (**3**), $[Cd(Br)_2(L^5)]_2{\cdot}2CH_3CN$ (**5**), $[Cd(Cl)_2(L^6)]_2$ (**7**), $[Cd(I)_2(L^3)]_2$ (**8**) and $[Cd(I)_2(L^6)]_2$ (**12**) are the same and are illustrated in figure S1. The numbering scheme for the halides and L are as shown for **1**.

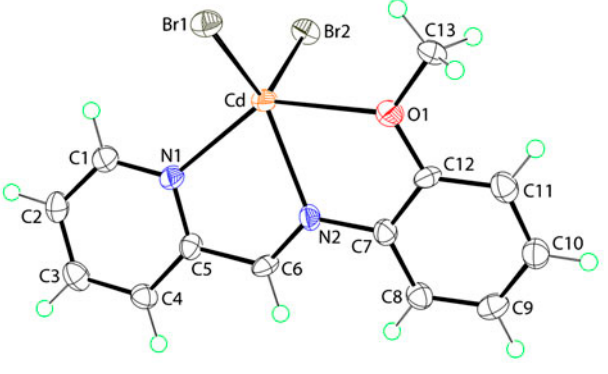

Figure 2. Molecular structure of mononuclear $[Cd(Br)_2(L^4)]$ (**4**).

coordinating ability of L^2 and L^3 compared with L^1, owing to the presence of methyl substituents in the former [47]. Systematic variations in the Cd–N bond lengths cannot be delineated with confidence, owing to the relative high errors associated with these parameters.

When the methyl substituent in L^2 is replaced by a methoxy group to give L^4, a major structural change occurs, owing to the coordination of the methoxy-O1 atom to cadmium (figure 2). In **4**, the five-coordinate donor set is based on a Br_2N_2O environment that defines a distorted square pyramidal geometry ($\tau = 0.10$) with the apical position occupied by the Br2 atom. The Cd–Br bond lengths differ by only 0.028 Å and are comparable with the terminal Cd–Br bond length in **1**; the Cd–N bond lengths are similarly equivalent. The second chelate ring formed owing to the interaction of the methoxy atom is non-planar and best

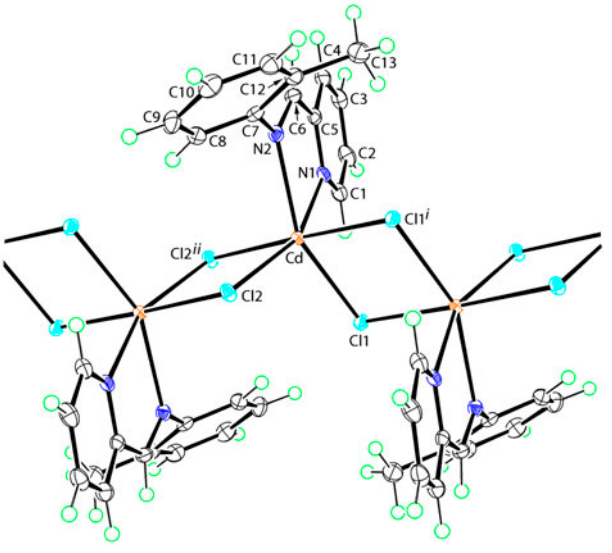

Figure 3. A segment of the polymeric structure in $[Cd(Cl)_2(L^2)]_n$ (**6**). Symmetry operations *i*: $1-x$, $1-y$, $1-z$ and *ii*: $2-x$, $1-y$, $1-z$.

described as an envelope with the Cd atom being the flap atom; the dihedral angle between the five-membered rings is 12.8(3)°.

The structure of **5** crystallized about a center of inversion along with a solvent acetonitrile molecule so that the overall composition is $[Cd(Br)_2(L^5)]\cdot 2CH_3CN$ (figure S4). The binuclear structure of **5**, with a methoxy group in the 4-position, resembles that of **3** but with a small elongation in Cd–Br1 which is compensated by a small reduction in the Cd–Br1^i bond length, Δ(Cd–N) = 0.146 Å; τ = 0.60. Only one structure containing $CdCl_2$ was obtained that is directly comparable with the aforementioned $CdBr_2$ structures, namely $[Cd(Cl)_2(L^2)]_n$ (**6**) (figure 3). A segment of the polymeric structure of $[Cd(Cl)_2(L^2)]_n$ (**6**) is shown in figure 3. The cadmium atom is chelated by L^2 and surrounded by four μ_2-chloro ligands with the resulting Cl_4N_2 donor set defining a distorted octahedral geometry. Pairs of bridging μ_2-chloro ligands bridge differently with one almost being symmetric but the other with a disparity in the Cd–Cl bond lengths, Δ(Cd–Cl) = 0.076 and 0.175 Å, respectively. The presence of stronger Cd–Cl bonds compared with Cd–Br bond in **2** results in a general elongation of the Cd–N bond lengths in **6** compared with those in **2**. The formation of a polymer in **6** and not in **2** can be correlated with the greater electronegativity of chloride over bromide which enhances the Lewis acidity of the cadmium atom which compensates by forming intermolecular interactions. The polymeric structure with a zigzag topology comprises edge-shared polyhedra propagated along the *a*-axis. While it was not possible to isolate crystals of a compound formed between $CdBr_2$ and L^6, crystals of the 1 : 1 compound with $CdCl_2$ were characterized as $[Cd(Cl)_2(L^6)]_2$ (**7**).

The molecular structure of binuclear $[Cd(Cl)_2(L^6)]_2$ (**7**), figure S4, resembles closely that of binuclear species described above. The Cd–Cl bridges are not symmetric with Δ(Cd–Cl) = 0.138 Å and the value of τ = 60. The question arises as to why this species is binuclear rather than polymeric as for **6** – a possible answer lies in the relative coordinating abilities of L. In **6**, the L^2 ligand, with an electron-donating methyl group chelates the

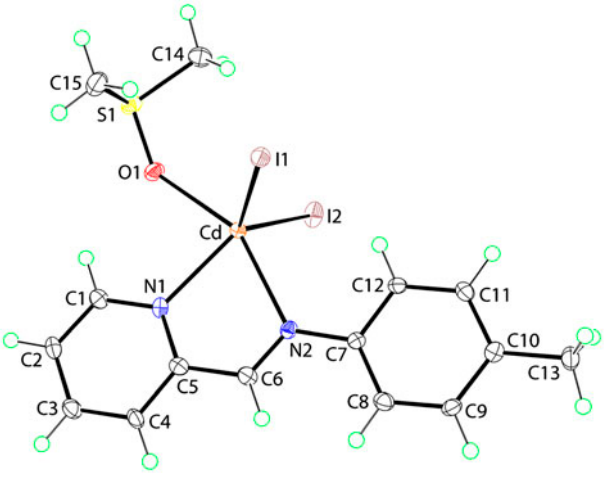

Figure 4. Molecular structure of mononuclear $[Cd(I)_2(L^3)(DMSO)]$ (**9**).

cadmium center relatively strongly, as established above for the $CdBr_2$ structures. This, in turn, reduces the strength of the Cd–Cl bonds. The chloro ligands in **6** compensate by bridging. Attention is now directed to the five crystal structure determinations featuring CdI_2.

Allowing for elongation of the Cd–I bond lengths, the pattern of geometric parameters describing the coordination geometry in $[Cd(I)_2(L^3)]_2$ (**8**), figure S4, follows that established for **3**; Δ(Cd–I) = 0.125 Å; τ = 0.46. While **8** was isolated from an acetonitrile/chloroform (*v*/*v*, 3 : 1) solution, when crystallization was from acetonitrile/dimethylsulfoxide (*v*/*v*, 6 : 1), mononuclear $[Cd(I)_2(L^3)(DMSO)]$ (**9**), figure 4, was isolated. The DMSO molecule coordinates via the O atom and the ensuing I_2 N_2O donor set in **9** defines a geometry almost intermediate between square pyramidal and trigonal bipyramidal with τ = 0.48.

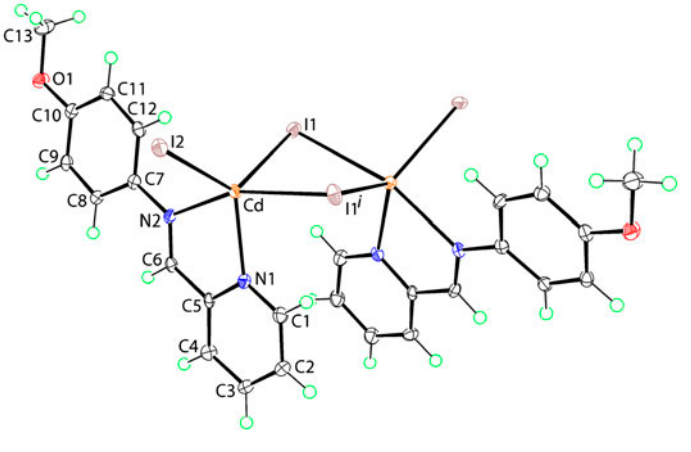

Figure 5. Molecular structure of binuclear $[Cd(I)_2(L^5)]_2$ (**11**). Unlabeled atoms are related by the symmetry operation $1 - x, y, \frac{1}{2} - z$.

Unlike the five-coordinate structure $[Cd(Br_2)(L^4)]$ (**4**), there is only a small difference in the Cd–I bond lengths in **9**, 0.01 Å; the Cd–N bond distances retain their expected disparity.

A five-coordinate geometry is also found in the structure of $[Cd(I)_2(L^4)]$ (**10**), figure S4, a direct analog of $[Cd(Br)_2(L^4)]$ (**4**), owing to the coordination of the methoxy-O atom in the 2-position of the aryl ring. The I_2N_2O donor set defines a geometry based on a square pyramidal with $\tau = 0.03$ with the I1 atom occupying the apical position. The $CdOC_2N$ chleate has an envelope conformation with the Cd atom being the flap atom; the dihedral angle between the five-membered rings is 13.5(3)°. As with **4**, but in contrast with all other structures reported herein, the Cd–N bond lengths in **10** are experimentally equivalent. The difference occurs as the Cd–N(imino) bond lengths contract in **4** and **10**, an observation correlated with the fact that the N(imino) is no longer *trans* to a halide atom as in the remaining structures.

The final two structures to be described are binuclear. The structure of $[Cd(I)_2(L^5)]_2$ (**11**), figure 5, stands out in that the molecule has crystallographic twofold symmetry rather than being centrosymmetric as for the other binuclear structures. The key structural consequence is that the terminal halide atoms are approximately *syn* as opposed to *anti* as found in the centrosymmetric structures. As the ligand L^5 is found in a structure with an *anti* conformation, i.e. **5**, and the remaining binuclear CdI_2 structures also adopt *anti* conformations, no obvious explanation is apparent for the adoption of the *syn* conformation in **11**. Other than this conformational difference, there are no significant differences in geometric parameters that are evident; Δ(Cd–I) = 0.250 Å and $\tau = 0.63$. The structure of $[Cd(I)_2(L^6)]_2$ (**12**), figure S4, conforms to the generally observed centrosymmetric binuclear motif with Δ(Cd–I) = 0.168 Å and $\tau = 0.48$. The unexpected observation for **11**, notwithstanding the fact that **12** and that of the $CdCl_2$ analog **7** both adopt the same structural motif, suggests that the $CdBr_2$ analog is likely to have the same structure.

A search of the Cambridge Structural Database [64] indicates that when complexed, molecules L^1–L^6 are invariably chelating. With the exception of the recent systematic study of mercury analogs [47], there are only three other literature precedents of these molecules with the zinc-triad elements. Each of the zinc compounds, i.e. $[Zn(Cl)_2(L^1)]$ [65] and $[Zn(I)_2(L^1)]$ [66], is mononuclear and the sole mercury structure is binuclear, i.e. $[Hg(Cl)_2(L^1)]$ [67]. Even from this limited database, some conclusions may be proffered. Thus, ZnX_2 compounds with L^n are likely to be mononuclear while those of CdX_2 and HgX_2 are generally more likely to increase the coordination number of the central atom via halide bridges to form binuclear species. The trend to aggregate increases in the order Cl > Br > I, a trend related to the electronegativity of the halide, as discussed above.

While there are no related crystal structures of the general formula $[M(X)_2(L^n)]$, where M is any heavy element and X is a halide for n = 1–3, examples do exist when n = 4–6. Thus, when n = 4, a five-coordinate copper(II) complex, $[Cu(Cl)_2(L^4)]$ [68], resembles closely that reported above for $[Cd(Br)_2(L^4)]$ (**4**). Two examples exist for L^5. Binuclear $[Cu(I)_2(L^5)]_2$ [69] resembles $[Cd(I)_2(L^5)]_2$ (**11**) but has an *anti* conformation of the L^5 ligands, rather than *syn* as in **11**. The second literature structure with L^5 is mononuclear and square planar $[Pt(Cl)_2(L^5)]$ [70]. Finally, mononuclear and square planar $[Pt(Cl)_2(L^6)]$, isolated as an acetonitrile solvate [71], contrast each of binuclear $[Cd(Cl)_2(L^6)]_2$ (**7**) and $[Cd(I)_2(L^6)]_2$ (**12**).

3.4. *Supramolecular aggregation*

The crystal packing of **1** is dominated by π…π interactions with the resulting supramolecular architecture being a 2-D array in the *ab*-plane (figure 6). The closest of these interactions

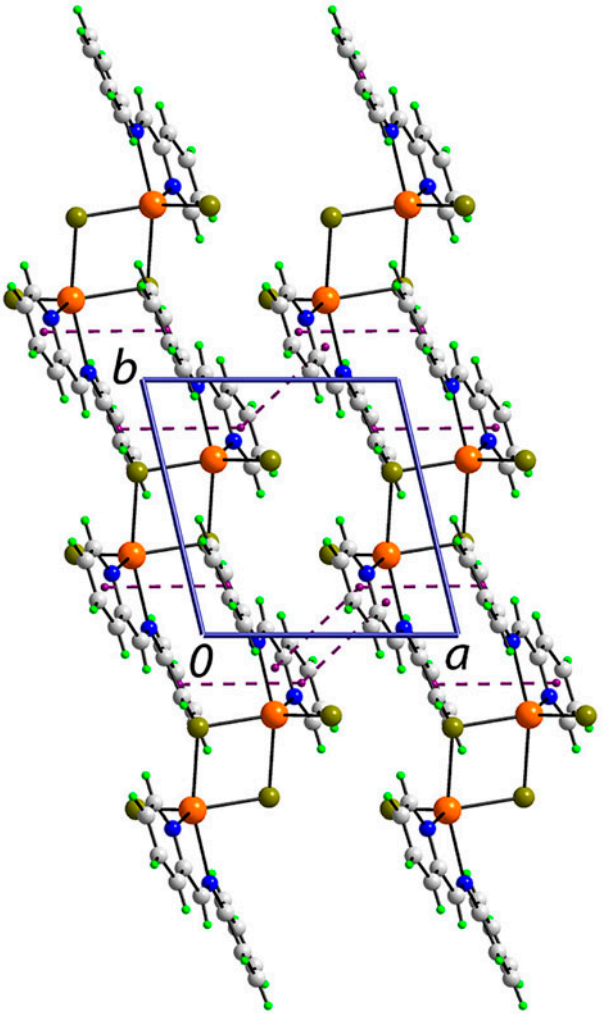

Figure 6. A view of the supramolecular layer in the *ab*-plane in **1**. The π…π interactions are indicated as purple dashed lines. For the (Cd, N1, N2, C5, C6) and (N1, C1–C5)^{i} rings, the inter-centroid distance = 3.756(3) Å, the angle of inclination between the rings = 4.8(3)° for symmetry operation *i*: $1-x, -y, 1-z$. For the (N1, C1–C5) and (C7–C12)^{ii} rings, inter-centroid distance = 3.904(4) Å, angle of inclination = 12.1(3)° for symmetry operation *ii*: $2-x, -y, 1-z$ (see http://dx.doi.org/10.1080/00958972.2013.864393 for color version).

[3.756(3) Å] occurs between the chelate ring and the pyridyl ring; geometric details are given in the caption to figure 9. Increasingly, such interactions involving chelate rings, having metallaromatic character [72], are appreciated as being important in stabilizing the crystal structures containing metal chelates [73, 74]. Complementing these interactions are contacts between the pyridyl and phenyl rings. In the crystal structure, the aryl rings projecting to either side of the layers partially inter-digitate along the *c*-axis, see ESI figure S5. Compound **8** is isostructural with **1** and details are included in ESI figure S6.

The structure of binuclear **2** was characterized as its benzene monosolvate. Molecules aggregate into a supramolecular chain along the *a*-axis via C–H…Br and C–H…π

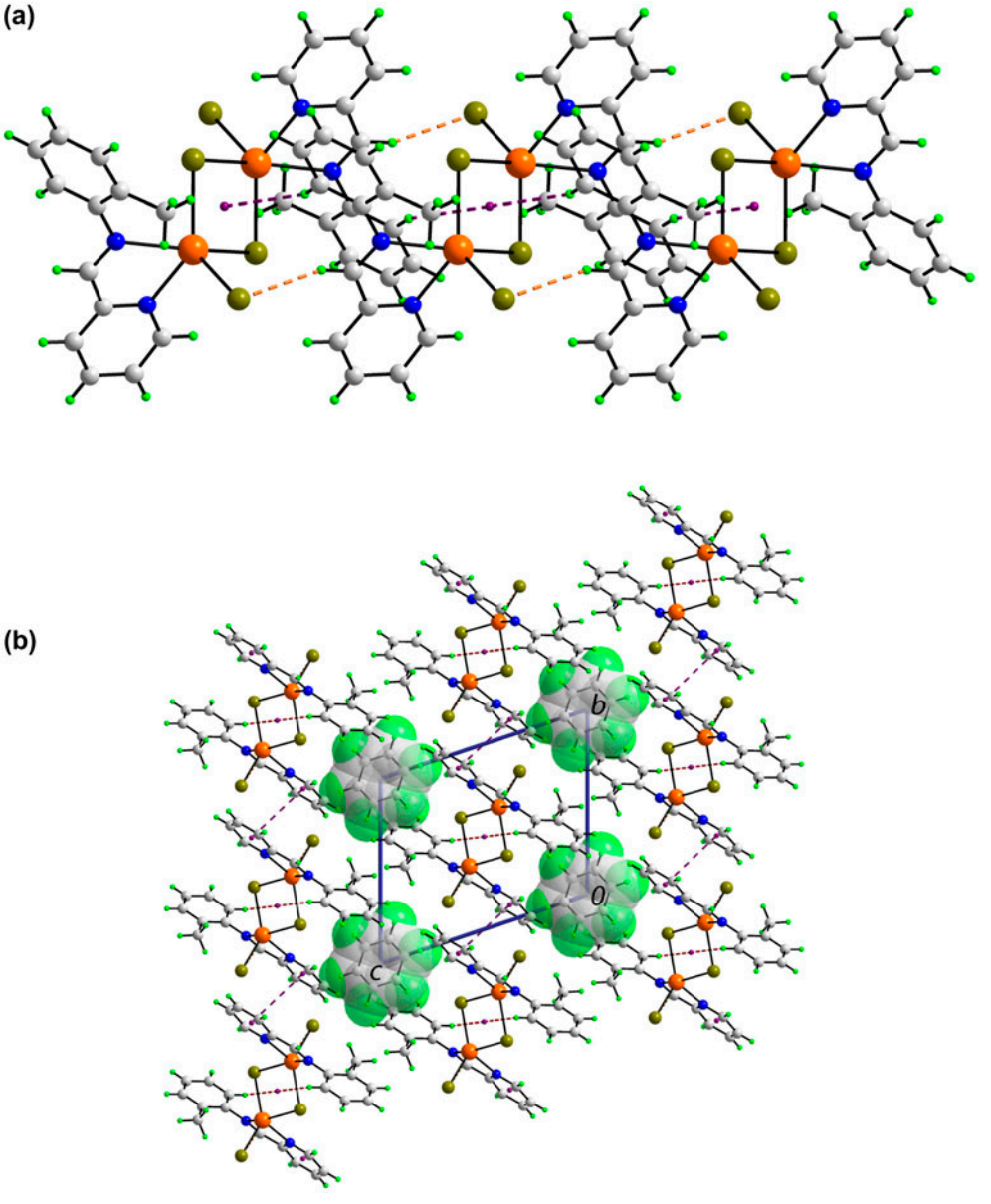

Figure 7. Crystal packing for **2**. (a) Supramolecular chain along the *a*-axis sustained by C–H...Br [C6–H6...Br2^{i} = 2.80 Å, C6...Br2^{i} = 3.699(2) Å and angle at H6 = 157° for symmetry operation *i*: −1 + *x*, *y*, *z*] and C–H...π [C8–H8...Cg(Cd_2Br_2)^{i} = 2.89 Å, C8...Cg(Cd_2Br_2)^{i} = 3.768(3) Å with angle at H8 = 154°] interactions shown as brown and brown dashed lines, respectively. (b) View of the unit cell contents in projection down the *a*-axis, the direction of the supramolecular chains, highlighting the formation of columns in which resides the solvent benzene shown in a space-filling mode. The π...π interactions [(N1,C1–C5) and (N1,C1–C5)^{ii} rings, inter-centroid distance = 3.8755(16) Å, angle of inclination = 0° for symmetry operation *ii*: −*x*, 1 − *y*, 1 − *z*] are shown as purple dashed lines (see http://dx.doi.org/10.1080/00958972.2013.864393 for color version).

interactions (figure 7(a)). In this case, the π-system is the Cd_2Br_2 ring which, having metalloaromatic character, is capable of forming such interactions [74, 75]. Chains are linked into layers in the *ab*-plane by π…π interactions between the pyridyl rings. While there are no specific interactions between the layers and benzene molecules, the columns in the crystal defined by the partially inter-digitating layers accommodate the benzene molecules (figure 7(b)).

The 3-D architecture in **3** is constructed by a combination of C–H…Br interactions involving the H3 and H6 atoms of L^3 connected to two different Br atoms, as well as two distinct π…π interactions occurring between the pyridyl and tolyl rings. The unit cell contents are illustrated in figure S7. While **3** has a methyl group in the 4-position of the aryl ring, substitution by chloride does not change the crystal packing in isostructural **7** (figure S8). Compound **12** is also isostructural but in this case, further stabilization to the crystal structure is provided by an additional C–H…Cl interaction involving a hydrogen atom already interacting with an iodide so that this atom (H3) is bifurcated as detailed in figure S9.

Thus, in isostructural **3**, **7**, and **12** different points of contact are identified based on the geometric parameters encompassed in PLATON [51]. The isostructural behavior, despite the presence of varying supramolecular synthons, points to the importance of global crystal packing of the molecules, i.e. close packing of irregularly shaped

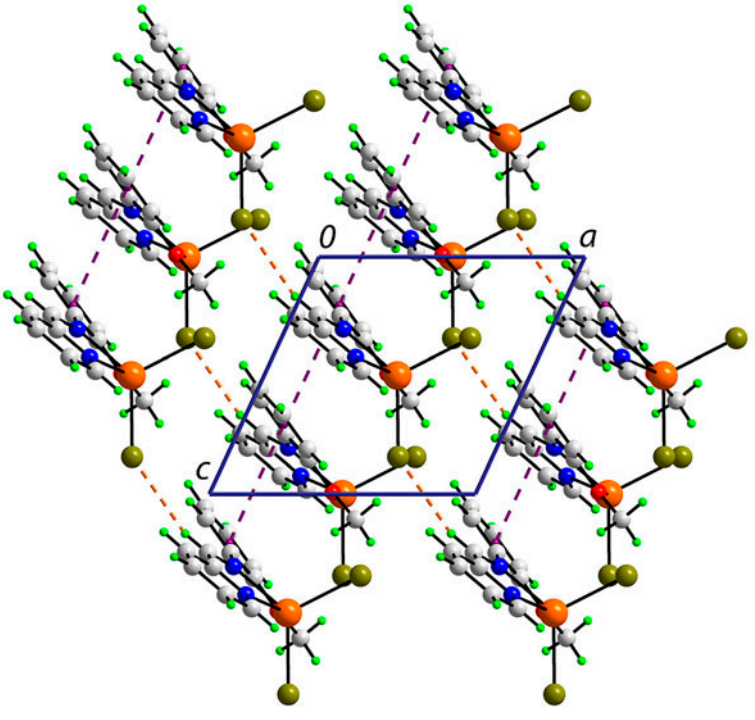

Figure 8. The supramolecular array in the *ac*-plane for **4** sustained by C–H…Br [C6–H6…Br1^{i} = 2.90 Å, C6…Br1^{i} = 3.800(7) Å and angle at H6 = 158° for symmetry operation *i*: −1 + *x*, *y*, −1 + *z*] and π…π [(C7–C12) and (C7–C12)^{ii} rings the inter-centroid distance = 4.065(4) Å, the angle of inclination between the rings = 12.8(3)° for symmetry operation *ii*: *x*, −*y*, −½ − *z*] interactions, indicated as orange and purple dashed lines, respectively (see http://dx.doi.org/10.1080/00958972.2013.864393 for color version).

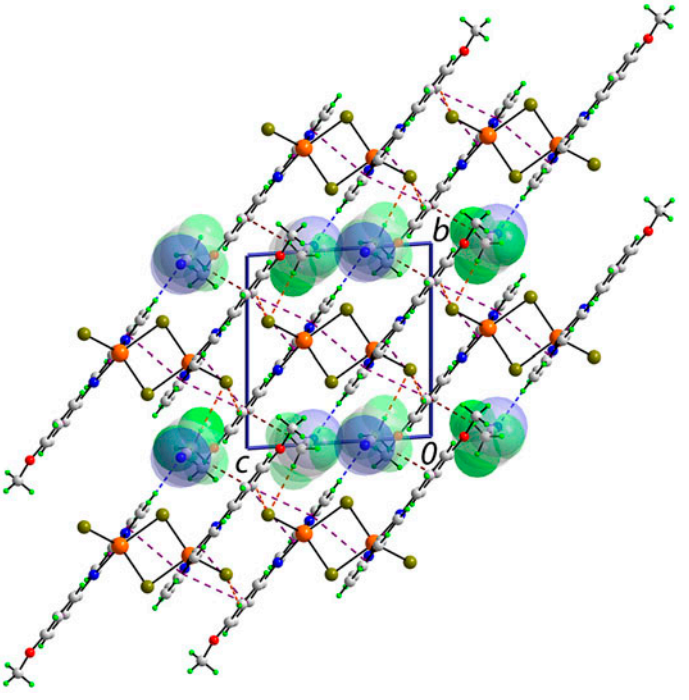

Figure 9. Unit cell contents for **5** viewed in projection down the *a*-axis. The C–H. . .Br [C11–H11. . .Br2^{i} = 2.93 Å, C6. . .Br2^{i} = 3.737(3) Å and angle at H6 = 144° for symmetry operation *i*: $1-x$, $1-y$, $-z$; C15–H15a. . .Br2^{ii} = 2.84 Å, C11. . .Br2^{ii} = 3.789(3) Å and 144° for *ii*: $2-x$, $-y$, $1-z$], C–H. . .N [C2–H2. . .N3 = 2.47 Å, C2. . .N3 = 3.412(4) Å and 172°; C13–H13b. . .N3^{iii} = 2.58 Å, C13. . .N4^{iii} = 3.456(5) Å and H13b = 149° for *iii*: x, $1+y$, $-1+z$], C–H. . .π [C15–H15b. . .Cg(C7–C12)^{iv} = 2.63 Å, C15. . .Cg(C7–C12)^{iv} = 3.460(3) Å and angle at H15b = 142° for *iv*: $2-x$, $1-y$, $1-z$], and π. . .π [(Cd,N1,N2,C5,C6) and (C7–C12)^{v} rings the inter-centroid distance = 3.8996(16) Å, the angle of inclination between the rings = 8.21(12)° for *v*: $2-x$, $1-y$, −z; (N1,C1–C5). . .(N1,C1–C5)^{iv} = 3.6079(16) Å, angle = 0°; (N1,C1–C5). . .(C7–C12)^{v} = 3.5781(16) Å, angle = 5.49(13)°] interactions are shown as orange, blue, brown and purple dashed lines, respectively (see http://dx.doi.org/10.1080/00958972.2013.864393 for color version).

molecules [74, 76]. This conclusion is also borne out in the crystal packing of **4** and **10**. The structures of mononuclear **4** and **10**, featuring coordinated methoxy atoms, are isostructural. The key feature of the crystal packing is the formation of a supramolecular layer in the *ac*-plane through a combination of C–H. . .Br and weak π. . .π interactions, the latter occurring between phenyl rings, as detailed in figure 8; a view of the unit cell contents for **4** is shown in figure S10 and full details for **10** are given in figure S11. In **10**, the π. . .π interactions are weaker but an additional C–H. . .I interaction occurs, which provide some cohesion between layers.

The structure of binuclear **5** was characterized as its acetonitrile disolvate. A 3-D architecture sustained by C–H. . .Br and π. . .π interactions is formed and this defines channels running parallel to the *a*-axis. Inside these reside the acetonitrile molecules which are held in place by C–H. . .Br, C–H. . .π and C–H. . .N interactions (figure 9). It is noteworthy that one of the π. . .π contacts involves the chelate ring interacting with a phenyl ring.

The remaining three crystal structures are stand-alone in that they are not isostructural with other molecules reported herein. Nevertheless, a common feature of their crystal packing is the formation of 2-D arrays. The polymeric chains in **6** are connected to translationally

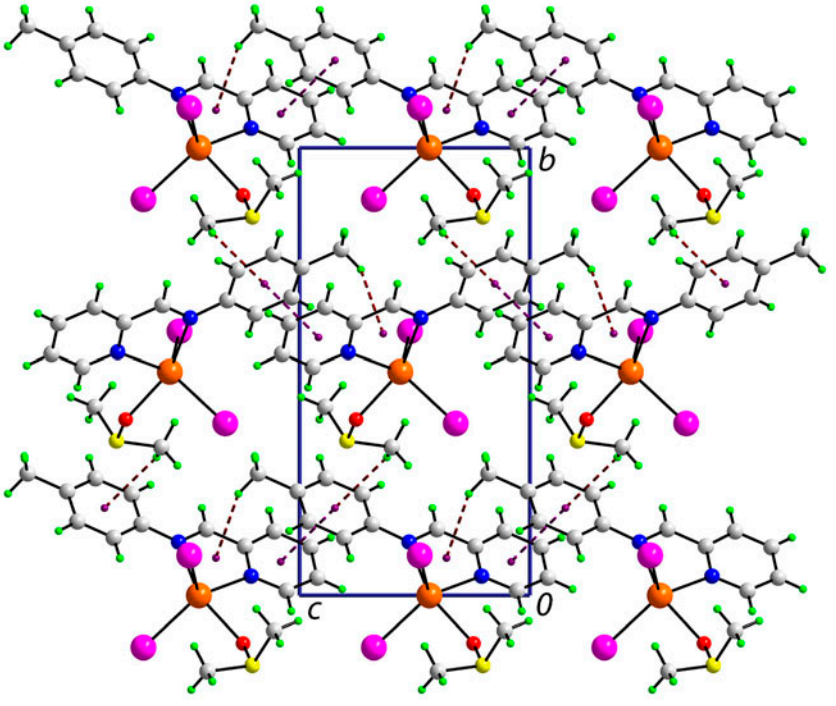

Figure 10. A view of the supramolecular array in the *bc*-plane for **9** sustained by C–H. . .π [C13–H13c. . .Cg(Cd, N1,N2,C5,C6)^{i} = 2.99 Å, C13. . .Cg(Cd,N1,N2,C5,C6)^{i} = 3.768(6) Å and angle at H13c = 138° for symmetry operation *i*: *x*, *y*, −1 + *z*; C14–H14c. . .Cg(N1,C1–C5)^{ii} = 2.92 Å, C13. . .Cg(Cd,N1,N2,C5,C6)^{ii} = 3.738(6) Å and angle at H14c = 142° for symmetry operation *ii*: −*x*, −½ + *y*, 1 − *z*] and π. . .π [(N1,C1–C5) and (C7–C12)^{iii} rings the inter-centroid distance = 3.594(3) Å, the angle of inclination between the rings = 4.7(3)° for symmetry operation *iii*: *x*, *y*, 1 + *z*] interactions, indicated as brown and purple dashed lines, respectively (see http://dx.doi.org/10.1080/00958972.2013.864393 for color version).

related chains along the *b*-axis by C–H. . .Cl and π. . .π [between tolyl rings] interactions to form a supramolecular layer in the *ab*-plane (figure S12(a)). Layers stack along the *c*-axis with no specific interactions between them (ESI figure S12(b)). The supramolecular array in the crystal structure of mononuclear **9** is sustained by C–H. . .π interactions whereby one DMSO-methyl group forms a contact with a pyridyl ring, and the tolyl-methyl forms a contact with the π-system defined by the chelate ring. Layers in the *bc*-plane are consolidated by π. . .π interactions between the pyridyl and tolyl rings (figure 10); the layers stack along the *a*-axis with no specific interactions between them (ESI figure S13). Finally, for **11**, the supramolecular array in the *ac*-plane is sustained by C–H. . .O and π. . .π interactions [between the pyridyl and tolyl rings], figure S14(a), and these stack along the *b*-axis with no specific interactions between them (ESI figure S14(b)).

4. Conclusions

A series of 12 cadmium compounds, $[Cd(X_2)(L)]$ (**4**, **10**), $[Cd(X_2)(L)(DMSO)]$ (**9**), $[Cd(X_2)(L)]_2$ (**1–3**, **5**, **7**, **8**, **11**, and **12**), and $[Cd(Cl_2)_2(L)]_n$ (**6**), where X = chloride, bromide, and iodide, and L = (*E*)-*N*-(pyridin-2-ylmethylidene)arylamine, were characterized. The $CdBr_2$ and CdI_2 compounds with L were usually binuclear unless additional donors on L or

solvent were able to coordinate with cadmium. Dimerization was only averted when L carries an oxygen donor capable of coordinating to cadmium or when coordinating solvent, i.e. DMSO, was present. In all cases, a five-coordinate cadmium environment ensued. While a binuclear structure was also observed for a sole $CdCl_2$ derivative, a polymeric structure with octahedral cadmium was found in one instance, i.e. $[Cd(Cl_2)_2(L)]_n$ (**6**), owing to the presence of μ_2-bridging chloro ligands, a result correlated to the presence of electronegative chloride coupled with a (relatively) strongly coordinating ligand, L. The detailed analysis of the crystal packing revealed the presence of unusual C–H. . .π interactions where the π-system is a chelate ring or a Cd_2Br_2 unit.

Supplementary material

CCDC numbers 913003–913014 contain the supplementary crystallographic data for **1–12**. These data can be obtained free of charge via http://www.ccdc.cam.ac.uk/conts/retrieving.html, or from the Cambridge Crystallographic Data Center, 12 Union Road, Cambridge CB2 1EZ, UK; Fax:+44 1223 336 033; or Email: deposit@ccdc.cam.ac.uk.

Acknowledgements

The financial support of the University Grants Commission, New Delhi, India (Grant No. 42-396/2013 (SR), TSBB) and that from the University Grants Commission, New Delhi, India through SAP-DSA, Phase-III are gratefully acknowledged. Support from the Ministry of Higher Education, Malaysia, High-Impact Research scheme (UM.C/HIR-MOHE/SC/03) is also gratefully acknowledged.

References

[1] C. Bianchini, G. Giambastiani, I. Guerrero Rios, G. Mantovani, A. Meli, A.M. Segarra. *Coord. Chem. Rev.*, **250**, 1391 (2006).
[2] C. Bianchini, D. Gatteschi, G. Giambastiani, I. Guerrero Rios, A. Ienco, F. Laschi, C. Mealli, A. Meli, L. Sorace, A. Toti, F. Vizza. *Organometallics*, **26**, 726 (2007).
[3] C. Bianchini, G. Giambastiani, I. Guerrero Rios, A. Meli, A.M. Segarra, A. Toti, F. Vizza. *J. Mol. Catal. A: Chem.*, **277**, 40 (2007).
[4] C. Bianchini, G. Giambastiani, G. Mantovani, A. Meli, D. Mimeau. *J. Organomet. Chem.*, **689**, 1356 (2004).
[5] C. Bianchini, G. Mantovani, A. Meli, F. Migliacci. *Organometallics*, **22**, 2545 (2003).
[6] A. Toti, G. Giambastiani, C. Bianchini, A. Meli, L. Luconi. *Adv. Synth. Catal.*, **350**, 1855 (2008).
[7] C. Bianchini, G. Giambastiani, L. Luconi, A. Meli. *Coord. Chem. Rev.*, **254**, 431 (2010).
[8] H. Chun, H. Jung. *Inorg. Chem.*, **48**, 417 (2009).
[9] A. Kuc, T. Heine, G. Seifert, H.A. Duarte. *Chem. Eur. J.*, **14**, 6597 (2008).
[10] S.Y. Lee, S. Park, H.J. Kim, J.H. Jung, S.S. Lee. *Inorg. Chem.*, **47**, 1913 (2008).
[11] E. Shyu, R.M. Supkowski, R.L. LaDuca. *Inorg. Chem.*, **48**, 2723 (2009).
[12] S. Takizawa, H. Somei, D. Jayaprakash, H. Sasai. *Angew. Chem. Int. Ed.*, **42**, 5711 (2003).
[13] S.J. Hong, J.Y. Ryu, J.Y. Lee, C. Kim, S.-J. Kim, Y. Kim. *J. Chem. Soc., Dalton Trans.*, 2697 (2004).
[14] S. Hasegawa, S. Horike, R. Matsuda, S. Furukawa, K. Mochizuki, Y. Kinoshita, S. Kitagawa. *J. Am. Chem. Soc.*, **129**, 2607 (2007).
[15] D.N. Dybtsev, A.L. Nuzhdin, H. Chun, K.P. Bryliakov, E.P. Talsi, V.P. Fedin, K. Kim. *Angew. Chem. Int. Ed.*, **45**, 916 (2006).
[16] G.A. Mines, B.-C. Tzeng, K.J. Stevenson, J. Li, J.T. Hupp. *Angew. Chem. Int. Ed.*, **41**, 154 (2002).
[17] A. Lan, K. Li, H. Wu, D.H. Olson, T.J. Emge, W. Ki, M. Hong, J. Li. *Angew. Chem. Int. Ed.*, **48**, 2334 (2009).
[18] L.-G. Qiu, Z.-Q. Li, Y. Wu, W. Wang, T. Xu, X. Jiang. *Chem. Commun.*, 3642 (2008).
[19] T. Gadzikwa, B.-S. Zeng, J.T. Hupp, S.T. Nguyen. *Chem. Commun.*, 3672 (2008).

[20] M.A. Withersby, A.J. Blake, N.R. Champness, P.A. Cooke, P. Hubberstey, W.-S. Li, M. Schroder. *Inorg. Chem.*, **38**, 2259 (1999).
[21] J. Yang, J.-F. Ma, Y.-Y. Liu, J.-C. Ma, S.R. Batten. *Cryst. Growth Des.*, **9**, 1894 (2009).
[22] Y.J. Lee, E.Y. Kim, S.H. Kim, S.P. Jang, T.G. Lee, C. Kim, S.-J. Kim, Y. Kim. *New J. Chem.*, **35**, 833 (2011).
[23] Z. Lin, M.-L. Tong. *Coord. Chem. Rev.*, **255**, 421 (2010).
[24] A.J. Blake, N.R. Brooks, N.R. Champness, P.A. Cooke, A.M. Deveson, D. Fenske, P. Hubberstey, M.J. Schroder. *J. Chem. Soc., Dalton Trans.*, 2103 (1999).
[25] Y.-Q. Huang, X.-Q. Zhao, W. Shi, W.-Y. Liu, Z.-L. Chen, P. Cheng, D.-Z. Liao, S.-P. Yan. *Cryst. Growth Des.*, **8**, 3652 (2008).
[26] H. Kwak, S.H. Lee, S.H. Kim, Y.M. Lee, E.Y. Lee, B.K. Park, E.Y. Kim, C. Kim, S.-J. Kim, Y. Kim. *Eur. J. Inorg. Chem.*, 408 (2008).
[27] R. Mondal, T. Basu, D. Sadhukhan, T. Chattopadhyay, M. Bhunia. *Cryst. Growth Des.*, **9**, 1095 (2009).
[28] G.R. Desiraju. *Acc. Chem. Res.*, **35**, 565 (2002).
[29] H.W. Roesky, M. Andruh. *Coord. Chem. Rev.*, **236**, 91 (2003).
[30] X.J. Luan, Y.-Y. Wang, D.-S. Li, P. Liu, H.-M. Hu, Q.-Z. Shi, S.-M. Peng. *Angew. Chem. Int. Ed.*, **44**, 3864 (2005).
[31] B.-B. Ding, Y.-Q. Weng, Z.-W. Mao, C.-K. Lam, X.-M. Chen, B.-H. Ye. *Inorg. Chem.*, **44**, 8836 (2005).
[32] C. Janiak. *J. Chem. Soc., Dalton Trans*., 2781 (2003).
[33] C. Hu, Q. Li, U. Englert. *CrystEngComm*, **4**, 20 (2002).
[34] C. Hu, Q. Li, U. Englert. *CrystEngComm*, **5**, 519 (2003).
[35] H.M. Park, I.H. Hwang, J.M. Bae, Y.D. Jo, C. Kim, H.-Y. Kim, Y. Kim, S.-J. Kim. *Bull. Korean Chem. Soc.*, **33**, 1517 (2012).
[36] H.-X. Guo, H.-B. Lin, Q.-H. Wang. *Acta Crystallogr., Sect. E*, **62**, m1239 (2006).
[37] C. Janiak, S. Deblon, H.-P. Wu, M.J. Kolm, P. Klüfers, H. Piotrowski, P. Mayer. *Eur. J. Inorg. Chem.*, 1507 (1999).
[38] H.-Y. He, Y.-L. Zhou, J. Chen, L.-G. Zhu. *Z. Kristallogr. New Cryst. Struct.*, **220**, 209 (2005).
[39] J. Sun, X. Tong, H. Xu. *Inorg. Chem. Commun.*, **13**, 645 (2010).
[40] H. Wang, R.-G. Xiong, H.-Y. Chen, X.-Y. Huang, X.-Z. You. *Acta Crystallogr., Sect. C*, **52**, 1658 (1996).
[41] Y.-H. Sun, S.-F. Luo, X.-Z. Zhang, Z.-Y. Du. *Acta Crystallogr., Sect. E*, **65**, m708 (2009).
[42] N. Kundu, D. Mandal, M. Chaudhury, E.R.T. Tiekink. *Appl. Organomet. Chem.*, **19**, 1268 (2005).
[43] Z.R. Ranjbar, A. Morsali, L.-G. Zhuz. *J. Coord. Chem.*, **60**, 667 (2007).
[44] W. Zhang, Z. Jiang, L. Lu. *Acta Crystallogr., Sect. E*, **65**, m7 (2009).
[45] K.-L. Zhong. *Acta Crystallogr., Sect. E*, **67**, m1609 (2011).
[46] J.-M. Shi, J.-N. Chen, L.-D. Liu. *Acta Crystallogr., Sect. E*, **62**, m2094 (2006).
[47] (a) T.S. Basu Baul, S. Kundu, S. Mitra, H. Höpfl, E.R.T. Tiekink, A. Linden. *Dalton Trans.*, 1905 (2013); (b) T.S. Basu Baul, S. Kundu, H. Höpfl, E.R.T. Tiekink, A. Linden. *Polyhedron*, **55**, 270 (2013).
[48] *CrysAlisPro (Version 1.171.33.55)*, Agilent Technologies, Yarnton, Oxfordshire, England (2010).
[49] G.M. Sheldrick. *Acta Crystallogr., Sect. A*, **64**, 112 (2008).
[50] L.J. Farrugia. *J. Appl. Crystallogr.*, **45**, 849 (2012).
[51] A.L. Spek. *Acta Crystallogr., Sect. D*, **65**, 148 (2009).
[52] K. Brandenburg. *DIAMOND*, Crystal Impact GbR, Bonn, Germany (2006).
[53] S.S. Tandon, S. Chander, L.K. Thompson. *Inorg. Chim. Acta*, **300–302**, 683 (2000).
[54] K. Nakamoto. *Infrared and Raman Spectra of Inorganic and Coordination Compounds*, Wiley, New York (1986).
[55] G. Mahmoudi, A. Morsali. *Polyhedron*, **27**, 1070 (2008).
[56] P. Biscarini, L. Fusina, G.D. Nivellini. *J. Chem. Soc., Dalton Trans*., 1003 (1972).
[57] K. Nakamoto. *Infrared and Raman Spectra of Inorganic and Coordination Compounds*, Part B, 6th Edn, Wiley, Hoboken, NJ (2009).
[58] (a) S.R. Li, L. Xu. *Inorg. Chem.*, **44**, 3731 (2005); (b) J. Lu, K. Zhao, Q.R. Fang, J.Q. Xu, J.H. Yu, X. Zhang, H.Y. Bie, T.G. Wang. *Cryst. Growth Des.*, **5**, 1091 (2005); (c) L. Wang, M. Yang, G.H. Li, Z. Shi, S.H. Feng. *Inorg. Chem.*, **45**, 2474 (2006); (d) K.L. Huang, Y.T. He, M. Huang. *J. Coord. Chem.*, **61**, 2735 (2008); (e) Y.L. Yao, L. Xue, Y.X. Che, J.M. Zheng. *Cryst. Growth Des.*, **9**, 606 (2009); (f) B. Liu, Y.C. Qiu, G. Peng, L. Ma, L.M. Jin, J.B. Cai, H. Deng. *Inorg. Chem. Commun.*, **12**, 1200 (2009).
[59] C.-C. Ji, L. Qin, Y.-Z. Li, Z.-J. Guo, H.-G. Zheng. *Cryst. Growth Des.*, **11**, 480 (2011).
[60] (a) A. Saha Roy, M.K. Biswas, T. Weyhermüller, P. Ghosh. *Dalton Trans.*, 146 (2011); (b) A. Saha Roy, P. Saha, P. Mitra, S.S. Maity, S. Ghosh, P. Ghosh. *Dalton Trans.*, 7375 (2011).
[61] A. Chakrabarty, S. Kar, D.N. Nath, N. Guchhait. *J. Phys. Chem. A*, **110**, 12089 (2006).
[62] S. Mahanta, R.B. Singh, S. Kar, N. Guchhait. *J. Photochem. Photobiol., A*, **194**, 318 (2008).
[63] A.W. Addison, T.N. Rao, J. Reedijk, J. van Rijn, G.C. Verschoor. *J. Chem. Soc., Dalton Trans.*, 1349 (1984).
[64] F.H. Allen. *Acta Crystallogr., Sect. B*, **58**, 380 (2002).
[65] K. Wurst, M.R. Buchmeiser. *Heterocycl. Commun.*, **5**, 37 (1999).

[66] (a) M. Schulz, M. Klopfleisch, H. Gorls, M. Kahnes, M. Westerhausen. *Inorg. Chim. Acta*, **362**, 4706 (2009); (b) J.J. Braymer, J.-S. Choi, A.S. DeToma, C. Wang, K. Nam, J.W. Kampf, A. Ramamoorthy, M.H. Lim. *Inorg. Chem.*, **50**, 10724 (2011).
[67] M.F. Nejad, M.R.T.B. Olyai, H.R. Khavasi. *Z. Kristallogr., New Cryst. Struct.*, **225**, 717 (2010).
[68] P.K. Bhaumik, S. Jana, S. Chattopadhyay. *Inorg. Chim. Acta*, **390**, 167 (2012).
[69] D.K. Seth, S. Bhattacharya. *Polyhedron*, **30**, 2438 (2011).
[70] S. Reinhardt, K. Heinze. *Z. Anorg. Allg. Chem.*, **632**, 1465 (2006).
[71] S. Dehghanpour, A. Mahmoudi, S. Rostami. *Polyhedron*, **29**, 2190 (2010).
[72] (a) H. Masui. *Coord. Chem. Rev.*, **219–221**, 957 (2001); (b) Y.Z. Wang, G.H. Robinson. *Organometallics*, **26**, 2 (2007).
[73] (a) Z.D. Tomić, D.N. Sredojević, S.D. Zarić. *Cryst. Growth Des.*, **6**, 29 (2006); (b) D.N. Sredojević, Z.D. Tomić, S.D. Zarić. *Cryst. Growth Des.*, **10**, 3901 (2010).
[74] E.R.T. Tiekink. In *Crystal Engineering in Supramolecular Chemistry: From Molecules to Nanomaterials*, J.W. Steed, P.A. Gale (Eds.), pp. 2791–2828, John Wiley & Sons, Chichester (2012).
[75] (a) M.K. Milčič, V.B. Medaković, D.N. Sredojević, N.O. Juranić, S.D. Zarić. *Inorg. Chem.*, **45**, 4755 (2006); (b) E.R.T. Tiekink, J. Zukerman-Schpector. *Chem. Commun.*, **47**, 6623 (2011).
[76] A. Gavezzotti. *CrystEngComm*, **15**, 4027 (2013).